Available online at www.sciencedirect.com
ScienceDirect
Journal of Molecular Graphics and Modelling 26 (2007) 104–116
Journal of Molecular Graphics and Modelling
www.elsevier.com/locate/JMGM

Structural, energetic, and dynamical properties of rotaxanes constituted of α-cyclodextrins and an azobenzene chain

Ludovic Briquet *, Nicolas Staelens, Laurence Leherte, Daniel P. Vercauteren [1]

Laboratoire de Physico-Chimie Informatique (PCI), University of Namur, 61 rue de Bruxelles, 5000 Namur, Belgium

Received 30 May 2006; received in revised form 9 October 2006; accepted 9 October 2006
Available online 13 October 2006

Abstract

The [3]rotaxane synthesised as a single isomer constituted of two cyclodextrins (CDs) and an azobenzene chain [M.R. Craig, T.D.W. Claridge, M.G. Hutchings, H.L. Anderson, Synthesis of a cyclodextrin azo dye [3]rotaxane as a single isomer, Chem. Commun. 16 (1999) 1537–1538] has been investigated using molecular mechanics (MM) and dynamics (MD) with the MM3 force field in order to evaluate the stability of various configurations of the complex in the isolated and solvated states. The influence of the blocking groups and the presence of energy barriers along the azo chain were first investigated through the calculation of an energy profile. It revealed that the CD could translate along the chain at room temperature without any decomplexation. Next, MD simulations of three different types of configurations, *i.e.*, head-to-head, head-to-tail, and tail-to-tail, of the [3]rotaxane were carried out. The non-solvated phase simulations showed structures with the CDs close to each other while the solvated ones showed structures with CDs separated by larger distances. This separation occurs due to the solute–solvent interactions. When the systems are in isolated state, the observed structure of the complexes are less stable due to an unfavourable arrangement of the hydroxyls groups of the adjacent CD faces. When considering solvation, energies of the three configurations are roughly identical due to the large distance between the faces of the CDs.

Keywords: Rotaxane; Cyclodextrin; Azobenzene; Molecular dynamics; Molecular mechanics; Energy profile

1. Introduction

For few decades, rotaxanes and related complexes have attracted much interest in supramolecular chemistry, especially as chemical mimics of biological systems, molecular machines, or for information storage. A [*n*]rotaxane is a molecule composed of $n - 1$ macrocycles which encircle a dumbbell-shaped component. The molecular components are not covalently linked and bulky stoppers bound to the ends of the linear component prevent dissociation of the complex. Because the macrocyles are not covalently linked to the chain, rotaxanes can be used as molecular motors [1–4] or molecular switches [5–12].

Cyclodextrins (CDs) are macrocyclic structures used to synthetise rotaxanes [1,2,7,9,10,12–15]. CDs are well known cyclic oligosaccharides formed by 6, 7, or 8 α-D-glucose named α-, β-, or γ-CD, respectively [16]. Their average structure shows a C_x symmetry axis (x standing for the number of glucose units) whilst the most stable conformation presents a lower symmetry [17,18]. Due to the presence of primary and secondary hydroxyl groups pointing outside the cavity, the outer surface is hydrophilic whereas the inner surface, lined with inside pointing C–H groups and ether-like oxygens, is hydrophobic. Because of this particular property, CDs are able to complex various organic compounds in aqueous solution [19] and are of special interest in pharmacology [20,21] and supramolecular chemistry [2,22]. As depicted in Fig. 1, the two faces of a CD structure are differentiated through their size and the nature of the closest hydroxyl groups. The larger face is constituted of secondary hydroxyl groups and is called the tail, while the smaller face, constituted of primary hydroxyl groups, is called the primary face or head. Many interactions, such as hydrogen bonds, can occur between the faces of adjacent CDs [23]. For example, Topchieva et al. [24] determined two different arrangements of the α-CDs in the channel structure of α-CD/polyethylene glycol complexes. The most stable

* Corresponding author. Tel.: +32 81 725462; fax: +32 81 725466.
E-mail addresses: ludovic.briquet@fundp.ac.be (L. Briquet), Daniel.vercauteren@fundp.ac.be (D.P. Vercauteren).
[1] Tel.: +32 81 72 45 34; fax: +32 81 72 54 66.

1093-3263/$ – see front matter
doi:10.1016/j.jmgm.2006.10.001

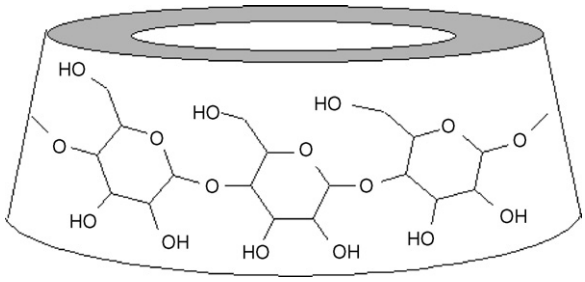

Fig. 1. Schematic representation of the truncated cone of α-CD.

arrangement presents a head-to-head/tail-to-tail sequence of CDs while the other structure adopts a head-to-tail configuration. Bonnet et al. [25] also showed through molecular dynamics (MD) simulation of CD dimers in vacuum and with solvent molecules, that the orientation of the CDs depends on the media. In the isolated state, the most stable orientation is tail-to-tail, whilst in water, the orientation is head-to-tail with perpendicular CDs and dominant solute-solute electrostatic interactions. Later a DFT study of α-CD dimer in water alters this conclusion [26]. Indeed, BLYP/6-31G(d,p)//PM3 calculations indicate that the tail-to-tail orientation of α-CDs is preferred by more than 10 kcal/mol in presence of water molecules. This structure presents five hydrogen bonds between the two α-CDs units forming the dimer and each α-CD possesses a water dimer inside its cavity and a water tetramer close to its head. Inclusion of the water tetramer between the α-CDs stabilize the head-to-head orientation only.

A family of organic molecules that are possible guests for CDs are azobenzenes [27–30]. The basic motif of these molecules is composed of two phenyl rings that are linked by an azo group, which leads to an enhanced electronic delocalisation over the whole system [31]. The *trans* to *cis* isomerisation of an azobenzene related molecule when complexed with a CD is a property that is often considered in molecular switch applications [10–14,28,29].

Regarding the encapsulation of chromophore molecules, Craig et al. first reported the synthesis of a [3]rotaxane constituted by an azobenzene chain and two α-CDs [14]. These authors described the preferred geometry of both the [3]rotaxane and the [2]rotaxane from ^{1}H NMR data. In the [3]rotaxane, the α-CDs are located at both ends of the linear chain and are exclusively ''head-to-head'' oriented, while in the [2]rotaxane, the CD is located head near a blocking group.

Few theoretical studies, mainly with molecular mechanics (MM) and MD, have been carried out on rotaxanes composed of CDs and azobenzene related molecules. We noted the studies of Barbiric et al. [32,33] who used the MM2 force field (FF) to understand the formation of 1:1 and 1:2 complexes between azobenzenes derivatives and β-CDs as well as to explain the experimentally observed inhibition of the thermal *cis–trans* isomerisation [28]. To investigate the isomerisation process of a molecular shuttle [12] composed of an azobenzene derivative and one α-CD, Sohlberg et al. [34] used the semi empirical AM1 approach to calculate the activation barrier of the isomerisation of the azo group, but severe convergence problems, caused by symmetry break, were mentioned. They concluded that the *cis* isomer is the most stable and that the isomerisation involves significant structural transformation, especially regarding the position of the α-CD along the chain.

More recently, several theoretical studies were carried out on systems containing CDs with other guest molecules. To determine the formation mechanism of the observed inclusion compound of *n*-alkyl carboxylic acids with α-CD [35,36], Lino et al. [37] applied the MM2, MM3, and OPLS FFs together with the GB/SA solvation model on several systems composed of α-CDs complexed with *n*-alkyl carboxylic acids and of β-CDs complexed with and *n*-alkyl *p*-hydroxy benzoate. They confirmed the experimental conclusions by determining the transition between 1:1 and 1:2 complexes at a length of $n = 9$. To study complexes between α-, β-, γ-CD and drug like molecules in aqueous solvents, Faucci et al. [38] used the AMBER FF. They especially focussed on the docking energy, intermolecular interaction fields, and host-guest surface contacts. Choi and Jung [39] used the MM Poisson–Boltzmann surface area approach and MD for the prediction of chiral discrimination of *n*-acetylphenylalanine by β-CD. They suggested that the conformational change of the guest due to the complexation with the β-CD is a determinant factor for the differentiation of the enantiomers.

The solvent effects on the structure and shuttling processes of rotaxane type compounds have not been intensively studied by theoretical chemists. We however noted the work of Jaime and collaborators who investigated the effect of implicit acetonitrile solvent [40] and explicit water and acetonitrile solvent [41,42] on a rotaxane structure composed by cyclobis-(paraquat-*p*-phenylene) macrocycle complexed to polymeric chain containing aromatic units. The force field MM3 was used for the investigation with GB/SA implicit solvation and AMBER was selected for explicit solvation studies.

In the present paper, we investigate the structural, energetic, and dynamical properties of the rotaxane structures described by Craig et al. [14], *i.e.*, α-CD complexed with 4,4′-[azobis(4,1-phenyleneazo)]bis[2,6-dimethylphenol], using the MM and MD program Tinker [43]. That particular system was selected due to the available description of the preferred geometries of the [3]- and [2]rotaxanes as reference data.

In Section 2, we define the molecular models that are used in this study and justify the choice of the FF. We also briefly describe the solvation method that was employed. Then, in Sections 3.1 and 3.2, we present the MM and MD studies of the [2]rotaxane. The ability of the blocking group to prevent the decomplexation of the α-CD is characterized and the movement of the α-CD along the chain is assessed. In Section 3.3, we examined three geometries of the [3]rotaxane, *i.e.*, head-to-head, head-to-tail, and tail-to-tail, and compared them with experimental data available from literature. Finally, MD simulations to examine the solvation effects on [3]rotaxane conformations are presented as well.

2. Methods

2.1. 3D-structure generation

The coordinates of the α-CD were taken from the Cambridge Structural Database (CSD) [44]. Among the α-CDs available in the database, we arbitrarily selected the compound referred to CHXAMH02 [45]. Starting from the compound referred as POXAW [46] in CSD, the 4,4′-[azobis(4,1-phenyleneazo)]bis[2,6-dimethylphenol] guest molecule was built using the *Materials Studio* building tools [47]. The α-CD and the guest molecule were then optimised separately with the PCFF *Materials Studio* FF [47]. A *steepest descent* algorithm was first considered with a convergence criterion of 1000.0 kcal/mol Å. It was followed by a *conjugate gradient* algorithm with 10.0 kcal/mol Å convergence and, finally, by a *quasi-Newton Raphson* algorithm with convergence = 0.1 kcal/mol Å. To generate the coordinates of the different models of the [2]- and [3]rotaxanes, one or two optimised α-CD molecules, respectively, were placed, at various locations, along the guest, as detailed further in the text. During all our calculations, with the exception of the energy profile, the entire inter- and intramolecular parameters were allowed to vary.

The MM simulations were carried out on a Pentium III 1 GHz processor and the MD simulations were run on a SUN i686 32 bits processor.

2.2. Force field selection

To select the FF that is appropriate for a complete study of the structural, energetic, and dynamical properties of the systems under interest, we tested CVFF [47] and PCFF [47] from *Materials Studio 3.0* using the *steepest descent*, *conjugate gradient*, and *quasi-Newton Raphson* optimisation algorithms, with a convergence threshold of 1000, 10, and 0.1 kcal/mol, respectively, and MM3 [48] from *Tinker 4.0* using successively the *Minimize* and *Optimize* algorithms with a convergence energy threshold of 0.1 and 0.001 kcal/mol. Starting from the XRD structures referred as AZOBEN03 [49] and AZOBENC01 [50] in CSD, we focussed on the ability of the FFs to reproduce the experimental geometry of *cis*- and *trans*-azobenzene, respectively. The geometrical parameters of the optimised structure, compared with available quantum mechanics and experimental data, are presented in Table 1; atom labels are shown in Fig. 2.

Optimised geometries for *trans*-azobenzene are very similar with all FFs. The N7–N8–C9–C14 angle is different from the XRD configuration (17.5°) but in agreement with DFT and MP2 calculations (0.0°).

Optimised geometries of the *cis*-azobenzene were observed to be rather dependent on the selected FF. CVFF led to a peculiar geometry where the phenyl groups seem to be mutually repulsed. Moreover, the configuration is flatter compared with the XRD data. This can be seen by the value of the N7–N8–C9–C14 and C2–N7–N8 angles that are considerably smaller (34.6°) and larger (135.6°) than the XRD values (53.3° and 121.9°), respectively. PCFF also presents a smaller dihedral N7–N8–C9–C14 angle (40.9°), but the difference is less pronounced than with CVFF. MM3 is more accurate in the description of the optimised azobenzene molecules. So considering these results, we used MM3, which include electronic delocalisation (remark: we considered nitrogen of type 37 in the FF), in the further investigations. Let us also note that the energy difference between the two isomers for MM3 (ΔE = 16.0 kcal/mol) is closer to the reported DFT calculation

Table 1
Principal geometrical parameters of the *trans*- (upper part) and *cis*-azobenzene (lower part) obtained from XRD, theoretical studies, and by geometrical optimisations with PCFF, CVFF, and MM3

	MP2/6-31 ++G(2d,2p) [31]	MP2/cc-pVTZ [51]	B3LYP/6-31 +G(d,p) [52]	X-ray [49]	PCFF	CVFF	MM3
N7–N8	127.1	126.8	125.8	124.7	128.3	122.7	127.4
C2–N7	142.1	141.7	142.0	142.8	139.7	142.0	142.5
C2–N7–N8	113.8	113.7	115.3	114.1	124.2	130.4	111.1
C3–C2–N7	115.0	115.1	115.3	115.6	120.0	117.8	118.2
C1–C2–N7	124.6	126.4	124.7	123.7	122.1	123.4	123.0
C2–N7–N8–C9	180.0	180.0	180.0	180.0	180.0	180.0	180.0
N7–N8–C9–C14	0.0	0.0	–	17.5	0.0	0.0	0.0
	DFT-BP86 [51]	MP2/cc-pVTZ [51]	B3LYP/6-31 +G(d,p) [52]	X-ray [50]	PCFF	CVFF	MM3
N7–N8	125.5	126.1	124.9	125.3	128.8	123.1	126.9
C2–N7	143.7	143.2	143.7	144.9	139.9	142.1	145.9
C2–N7–N8	124.1	120.8	124.0	121.9	128.6	135.6	119.9
C3–C2–N7	116.4	117.0	122.9	117.3	120.0	118.3	128.8
C1–C2–N7	122.9	122.2	116.5	122.5	122.0	122.6	117.2
C2–N7–N8–C9	11.4	7.3	9.5	8.0	9.9	6.3	10.8
N7–N8–C9–C14	48.4	53.6	50.9	53.3	40.9	34.6	54.3
$\Delta E_{cis/trans}$	–	–	15.5	–	6.1	7.0	16.0

The last line is the energy difference between the *trans* and *cis* isomers. Distances are in pm, angle in degrees, and energies in kcal/mol. Atom labels are presented in Fig. 2.

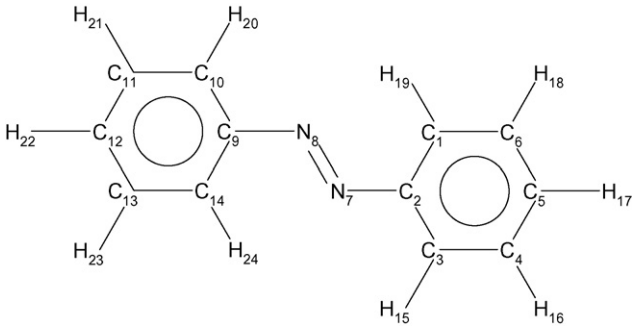

Fig. 2. Planar structure formula of *trans*-azobenzene with atom labels.

(ΔE = 15.5 kcal/mol) (Table 1). The other FFs provide smaller energy differences.

2.3. Energy profile calculation

In this section, we describe the method for the calculation of the energy profile obtained when the α-CD is translated along the guest chain. The algorithm used for these calculations is implemented in *Path* [53], a code included in the package *Tinker* [43]. Considering an initial and a final optimised configuration for the system, the final system is first superimposed on the initial one. Then, a trajectory is defined as:

$$\vec{\mathbf{r}}_\xi = \xi\vec{\mathbf{r}}_i + (1-\xi)\vec{\mathbf{r}}_\mathrm{p} \quad (1)$$

where ξ is a dimensionless reference coordinate which varies from 0 to 1 and $\vec{\mathbf{r}}_\xi$ is a configuration vector built on the *3N* coordinates of the *N* atoms of the system. At each step of the energy profile calculation, the system is optimised under constraints that are applied to avoid rigid body translation and rotation during energy minimization [53].

To define the initial configuration, the centre of mass (COM) of the α-CD was located at the level of the hydroxylated carbon of the phenyl group (Fig. 3). The α-CD has its tail near the blocking group. In the final configuration, the α-CD is placed at the other side of the chain with its head near the blocking group and with its COM located at the level of the hydroxylated carbon.

Each of the 76 configurations, that were generated between the initial and final configurations, were analysed so as to determine the intermolecular energy between the molecular partners (E_inter). E_inter was calculated from the total potential energy of the complex (E_complex), the individual potential energy of the host (E_CD), and the guest molecule (E_azo) according to:

$$E_\mathrm{inter} = E_\mathrm{complex} - E_\mathrm{guest} - E_\mathrm{CD} \quad (2)$$

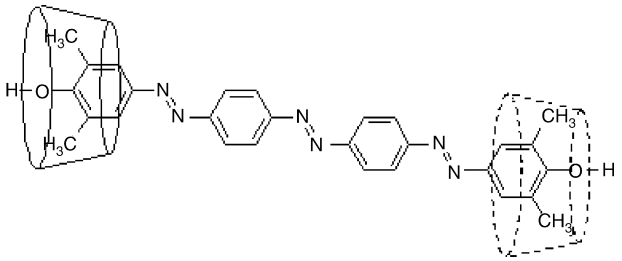

Fig. 3. Schematic representation of the initial configuration (plain line CD) and the final configuration (dotted line CD) for the energy profile calculation.

2.4. Molecular dynamics simulations

All the MD simulations consisted in an equilibrium and a production stage. The duration of the equilibrium dynamics was set equal to 20 ps and the temperature was chosen to be the experimental value, *i.e.*, 330 K [14]. All simulations were carried out in the canonical NVT ensemble. The selected time step was always set equal to 1 fs and coordinates and velocities were saved every 50 fs.

2.4.1. Molecular dynamics of the [2]rotaxane

The starting configuration for the simulation of a [2]rotaxane was the one at step 16 of the energy profile (*cf*. Section 3.1). It corresponds to an energy minimum with the tail of the α-CD located just on the right of the blocking group. The total simulation time of this MD run was set to 820 ps.

2.4.2. Molecular dynamics of the [3]rotaxane

Three types of structures were selected for the MD study of the [3]rotaxane, one where the α-CDs have their tail facing to each other, which we call tail-to-tail (T–T), one where the α-CDs are placed head-to-head (H–H), and the last one with the α-CDs in a head-to-tail (H–T) configuration. Two types of MD simulations were carried out for each configuration for a period of 102.5 ps, one in the isolated phase and another with a solvation model (*cf*. Section 2.5). An additional simulation was carried out for a period of 1 ns for the experimentally observed H–H complex with implicit solvation.

For each of the three configurations, two geometry optimisations were first carried out to determine the starting points of the dynamics. The starting configurations for the geometry optimisations were built using the *Materials Studio* [46] tools to place the COM of the α-CDs close to the middle of the N=N bond of the chain. More precisely, one set of coordinates was determined such as the α-CDs were placed around two successive azo bonds and a second set of coordinates was determined such as to place the α-CDs around the two end azo bonds. Geometry optimisations were then carried out with MM3 using successively the *Minimize* and *Pss* programs [54] with a convergence energy threshold of 0.1 and 0.0001 kcal/mol, respectively.

For each of the T–T and H–T complexes, we selected the most stable configuration as the starting point of the dynamics. For the H–H complex, we selected the structure where the α-CDs are well separated *versus* each other instead of the most stable one. The justification of this choice is discussed further in the paper.

2.5. Solvation method

Later in this work, we report results obtained from calculations that include solvation effects. These calculations

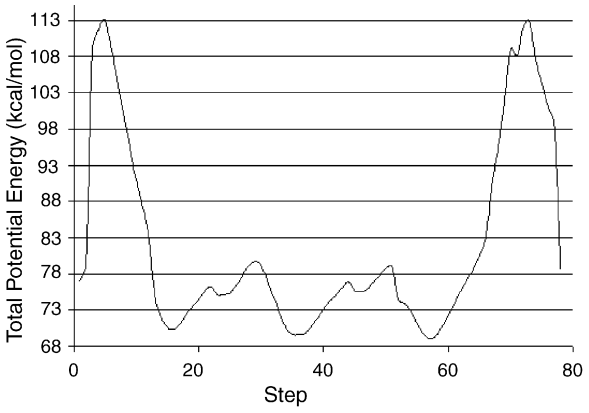

Fig. 4. Energy profile for the [2]rotaxane α-CD/azobenzene as observed between the configurations presented in Fig. 3. Calculations were performed with the TINKER routine *Path* and MM3 force field.

were achieved using the *Solvate ASP* [55] option available in *TINKER* [43]. In this method, a solvation energy term is added to the total potential energy. This solvation contribution to the energy (E_{solv}) is calculated as a sum over each atom (except hydrogens) of the atomic solvation parameter ($\Delta\sigma_i$) multiplied by an accessible surface term for the solvent (A_i):

$$E_{solv} = \sum_{i}^{n_{at}} \Delta\sigma_i A_i \quad (3)$$

The atomic solvation parameter represents the transfer energy of an atom from a non-solvated phase to a solvated phase. This parameter is tabulated for all atom types, except hydrogen [55].

3. Results and discussion

3.1. Energy profile of the [2]rotaxane

The energy profile generated by translating the α-CD along the guest chain was established to evaluate the efficiency, in term of energy barrier, of the end group of the chain as a blocking group, and to determine whether the motion of the α-CD along the guest molecule is energetically favourable.

The total energy profile is shown in Fig. 4. Selected energy values are presented in Table 2. Six maxima and five minima are visible on the profile. The two highest barriers located at both ends of the profile (steps 5 and 73) are attributed to the interaction of the α-CD with the blocking groups of the guest. The positive intermolecular energy, E_{inter}, at step 5 and the slightly negative one at step 73 are associated with very destabilizing van der Waals (vdW) energy components corresponding to a major steric effect of the blocking groups. These two maxima of more than 45 kcal/mol illustrate the role of the blocking groups in term of energy barrier; this barrier of decomplexation of the system cannot be passed at room temperature.

The two intermediate maxima, $\Delta E = 10.1$ kcal/mol, at steps 29 and 51 correspond to the interaction of the α-CD with the two middle phenyl groups whereas the three minima at step 16, 36, and 57 correspond to the interaction with each of the three azo double bonds, respectively. The E_{inter} values reported in Table 2 show that the main component of the intermolecular energy is the vdW term, $E_{vdW\text{-}inter}$, while the dipole–dipole (electrostatic) component, $E_{dip\text{–}dip\text{-}inter}$, is only slightly stabilizing and rather constant along the whole profile. The $E_{dip\text{–}dip\text{-}inter}$ variation along the whole profile is below 4.7%. Another energy component that participates to most of the total energy $E_{complex}$ variation is the potential energy of the α-CD, E_{CD}. Actually, large variations of $E_{complex}$ are correlated with changes of the α-CD potential energy. Indeed, the α-CD deforms when translating along the chain. This is illustrated in Table 3 where the mean and the standard deviation values of several bond lengths and angles of the α-CD and of the guest are presented. For the guest, we report the N=N and C–N distances and the C–C–N and C–N=N angle values, while for the α-CD, we report the distances between opposite O atoms and O–O–O angle values (Fig. 5). The geometrical parameters of the azo guest chain are quite constant, with a small standard deviation value, but the parameters that characterize the cavity size of the α-CD show larger standard deviation values. The differences between the three calculated internal diameters of the α-CD indicate that it adopts an oval form at all locations along the guest chain (Fig. 5).

The four intermediate maxima, at steps 22, 29, 44, and 51, are paired. Between the first two and the last two maxima, there are two shallow minima, which correspond to stable configurations with the α-CD placed at the level of the phenyl group. These two configurations are stabilized by weak interactions between the primary hydroxyl groups of the α-CD face (head) and the *N* atoms of the azo group.

The most stable configuration of the complex is observed at step 57 (Fig. 5), where the α-CD has its head near a blocking group. This observation is in agreement with the ‘‘qualitative’’ structure proposed by Craig et al. [14]. The stronger stability is

Table 2
Energy terms (kcal/mol) at selected steps of the energy profile of the [2]rotaxane, largest corresponding variations, and average energies calculated from the MD simulation for a period of 820 ps, carried out at 330 K, in the NVT ensemble using the TINKER routines *Path, Analyze*, and *Dynamic* and MM3 force field

	5	16	22	29	36	44	51	57	73	ΔE_{max}	MD
$E_{complex}$	113.1	70.5	75.2	79.7	69.6	75.5	78.9	69.0	112.8	±44.0	271.0 ± 7.9
E_{guest}	39.9	34.5	34.4	39.4	34.2	34.4	34.4	34.5	40.5	±6.3	113.2 ± 5.4
E_{CD}	70.9	55.2	56.4	56.9	54.7	56.3	57.0	54.6	74.2	±17.9	176.9 ± 7.4
E_{inter}	2.3	−19.4	−15.5	−11.6	−19.3	−15.2	−12.5	−20.1	−1.9	±22.4	−19.3 ± 2.3
$E_{vdW\text{-}inter}$	2.9	−18.9	−15.1	−11.1	−18.3	−14.8	−11.8	−19.0	−0.5	±21.9	−18.0 ± 1.9
$E_{dip\text{–}dip\text{-}inter}$	−0.6	−0.5	−0.4	−0.5	−1.0	−0.4	−0.6	−1.1	−1.5	±1.0	−1.3 ± 0.8

ΔE_{max} stands for the difference between the highest and lowest energy value observed along the profile.

Table 3
Average and standard deviation values of several geometrical parameters for the guest and the α-CD along the whole energy profile (calculations were performed with the TINKER routine *Path* and with MM3 force field)

	Distances (pm)	Angles (°)
Guest	R_{NN}: 126.9 ± 0.1	A_{CCN}: 121.0 ± 0.5
	R_{CN}: 138.0 ± 1.0	A_{CNN}: 111.8 ± 1.1
CD	R_1: 855.6 ± 17.2	A_1: 112.1 ± 2.6
		A_2: 118.9 ± 1.8
	R_2: 906.1 ± 22.7	A_3: 128.0 ± 2.4
		A_4: 112.4 ± 2.3
	R_3: 783.2 ± 19.1	A_5: 119.0 ± 1.9
		A_6: 128.5 ± 2.6

Geometrical parameters of the α-CD are defined in Fig. 5.

attributed to the freedom of motion of the primary alcohol functions of the α-CD head *versus* the secondary ones. Although $E_{dip–dip-inter}$ is rather constant along the whole profile, it is slightly more stable when the head of the α-CD is located near a blocking group due to more numerous interactions between the α-CD hydroxyl groups and the guest ones. In the configurations taken by the system between steps 16 and 57 (the two external minima), a smaller $E_{dip–dip-inter}$ value is explained by the hydrophobic property of the CD cavity. Indeed, in the framework of the MM3 FF [48], the chemical bonds that present a strong dipole moment are the bonds that are involved in the alcohol function of the guest, *i.e.*, C–O: 1.170 D and O–H: −1.670 D. The phenol bond dipole moments are weaker: C–O: 0.010 D; O–H: −0.700 D. C–N bonds also present a strong dipole moment (C–N: 1.290 D) but the chemical arrangement C–N=N–C is characterized by a very small resulting dipole moment; in addition, the dipole moment of the N=N bond is equal to zero.

3.2. Molecular dynamics of the [2]rotaxane

To further investigate the ability of a CD to cross intermediate maxima and to move along the chain, MD simulations of the [2]rotaxane were carried out. Average energy results of the MD simulations are presented in Table 2 and selected snapshots are shown in Fig. 6.

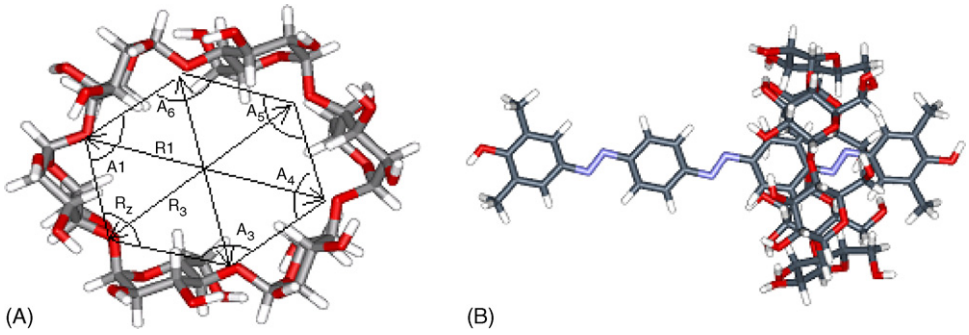

Fig. 5. Description of the CD shape (A) and general configuration (B) of the system as observed for the [2]rotaxane at step 57 of the energy profile calculation. Numerical values of the various distances and angles of the α-CD shape are presented in Table 3. Calculations were performed with the TINKER routine *Path* and MM3 force field.

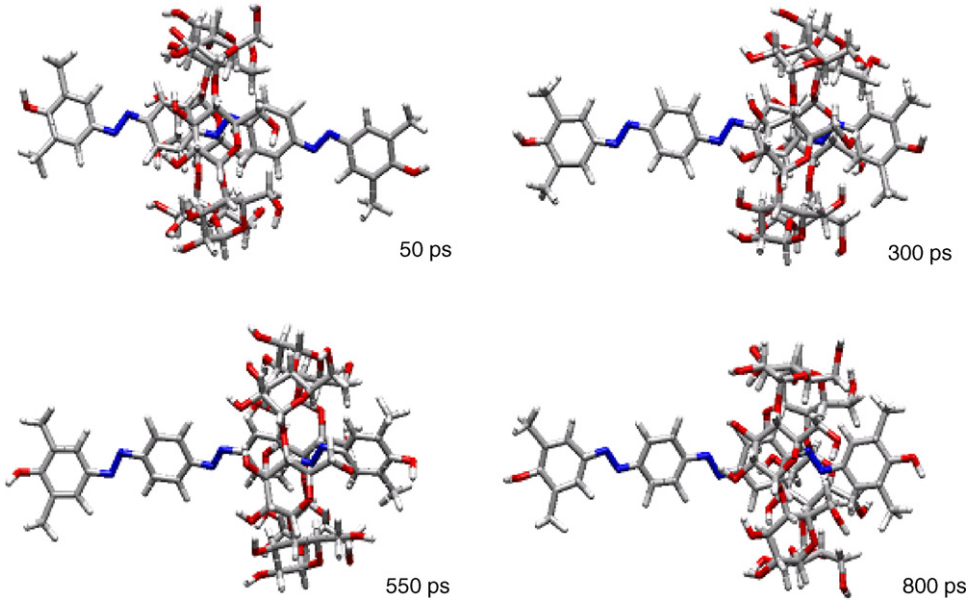

Fig. 6. Conformations adopted by the [2]rotaxane at simulation steps equal to 50, 300, 550, and 800 ps of the MD simulation carried out at 330 K, in the NVT ensemble, for a period of 820 ps, using the TINKER routine *Dynamic* and MM3 force field.

The analysis of the MD production stage showed that a translational motion is allowed at 330 K. At the beginning of the equilibrium dynamics, the α-CD was located at the position of the left minimum (step 16, *cf*. Section 2.4.1). At the end of the equilibrium stage, the CD was close to the middle minimum (step 36) observed in the energy profile (Fig. 4), which was considered as the initial configuration of the production stage. After about 190 ps, the α-CD has moved to a position corresponding to the right minimum (step 57) of the energy profile, *i.e*., a position when the primary face of the α-CD is close to the blocking group. To pass the maximum around step 51, the complex took a particularly distorted conformation, the α-CD being partially complexed with a phenyl group to allow a close contact between a primary hydroxyl group and a guest *N* atom (Fig. 7). These conformations corresponding to transition structure were adopted several times during the MD simulation for various periods of time. At time step equal to 150 ps, the complex remains in this conformation for a duration of 40 ps before passing in the other minimum. Later in the MD simulation, the complex adopts many times this organization, but only for short periods of time (1–5 ps). At time 620 ps, the complex re-adopts this particular conformation for a longer duration of 50 ps without passing in the other minimum.

When compared with the energy terms reported from the energy profile calculated at 0 K, the various mean energy contributions of the MD show very different values (Table 2). First of all, the total potential energy of the complex is at least twice higher at 330 K than at 0 K. This comes with high values of the individual potential energy of the α-CD and guest molecules, 176.9 and 113.2 kcal/mol, respectively. The intermolecular energy E_{inter} between both partners is of the same order of magnitude, −19.3 kcal/mol, than those observed in the minima of the energy profile. Decomposing E_{inter}, we observe an average vdW interaction energy part $E_{\text{vdW-inter}}$ during the MD simulation that is slightly higher than the one of the right minimum of the energy profile, −18.0 kcal/mol *versus* −19.0 kcal/mol, due to the transition structures of the MD. On the other hand, the average dipole–dipole energy part of the intermolecular energy $E_{\text{dip–dip-inter}}$ observed in the MD simulation is only slightly more negative than the value of the right minimum, −1.3 kcal/mol *versus* −1.1 kcal/mol. By analysing the evolution of $E_{\text{dip–dip-inter}}$ during the simulation

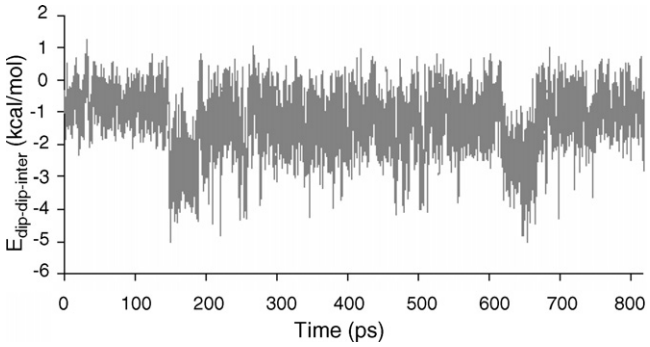

Fig. 8. Evolution of the dipole–dipole contribution of the intermolecular energy during the MD simulation carried out at 330 K, NVT ensemble, for a period of 820 ps, using the TINKER routine *Dynamic* and MM3 force field.

(Fig. 8), two different areas appear with an energy difference of roughly 2 kcal/mol, *i.e*., a variation that is higher than the standard deviation of $E_{\text{dip–dip-inter}}$ (0.8 kcal/mol). Structures with lower $E_{\text{dip–dip-inter}}$ contributions correspond to transition conformations for the crossing of the maxima, with the α-CD partially complexed with a guest phenyl group and in interaction with *N* atoms. These particular conformations are responsible of the more negative average $E_{\text{dip–dip-inter}}$ term.

To confirm the possible movement of the α-CD from a position that correspond to minimum in the energy profile to another energy minimum, two additional MD simulations were performed in the same conditions (temperature, simulation time, etc.) but with different starting points for the equilibrium dynamics, *i.e*., conformations at steps 36 and 57 of the energy profile. A similar behaviour was observed for the translation of the α-CD and for the interaction between the α-CD alcohol functions and the guest *N* atom in the transition structures.

In all these MD simulations, the guest chain never leaves the α-CD cone. This confirms the good stability of the complex at room temperature predicted by the previous energy profile calculations with a large energy barrier to the decomplexation of the rotaxane.

3.3. Molecular dynamics of the [3]rotaxane

In this part, we investigate the relative stability of the experimental configuration of the [3]rotaxane compared to

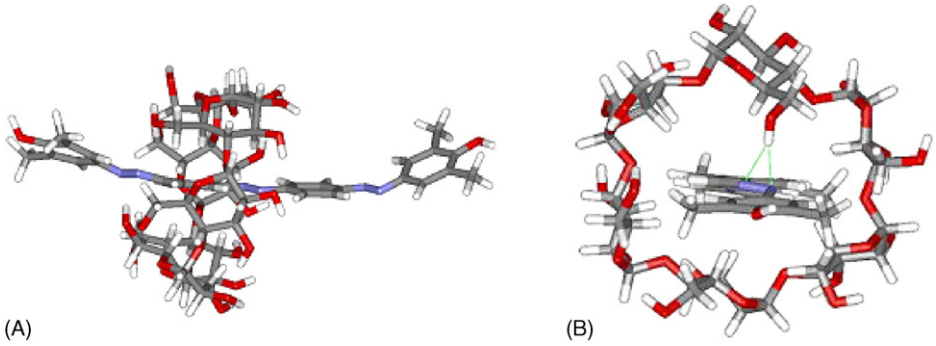

Fig. 7. Representation of a distorted structure of [2]rotaxane and interactions between primary hydroxyl groups and nitrogen atoms (dotted lines) that appear during the crossing of the energy barrier. These snapshots were taken at time 177 ps (A) and 183 ps (B) of the MD simulation carried out at 330 K, in the NVT ensemble, for a period of 820 ps, using the TINKER routine *Dynamic* and MM3 force field.

other hypothetical configurations and we explore the effect of the solvation on the relative stabilities. Therefore, many geometry optimisations of several configurations were carried out. The final optimised geometries let appear several interesting features. First, for head-to-head (H–H) complexes, the α-CDs remain approximately at the same position than in the starting structures, *i.e.*, when the α-CDs were both located around the azo bonds, they remained close to each other, and when they were close to the blocking groups, they remained next to them, like in the experimental complex. Second, for head-to-tail (H–T) complexes, the α-CDs, in both cases, converged to each other, with close contacts. Last, for tail-to-tail (T–T) complexes, the α-CDs converged to each other, as for the other configurations. It was established that when the α-CDs are in close contact, the hydroxyl groups self-organize to each other to lead to stabilizing electrostatic dipole–dipole interactions.

Energy values of the MD simulations are presented in Table 4 and selected snapshots are shown in Fig. 9. Simulations with solvent show more stable complexes than without solvation. The stabilization is due to the additional negative solvation energy term E_{solv}. If one removes E_{solv} from the potential energy E_{pot} to give $E_{non\text{-}solv}$, it shows that the structures of the non-solvated systems are more stable than the solvated ones. For example, $E_{non\text{-}solv}$ for H–H in solvated state is larger then E_{pot} for H–H in isolated state. The structure of the solvated complexes is distorted to allow stabilizing interactions with the solvent. The rather small energy deviation of E_{tot}, ±1.9 kcal/mol for the H–H complex in solvated state, originates from the compensation of large fluctuations observed in E_{pot}, 10.3 kcal/mol, and E_{kin}, 10.2 kcal/mol.

The three H–H, H–T, and T–T simulations without solvent showed the formation of dimers constituted by the two α-CDs. It was not observed for the systems with solvation due to an increase of the accessible surface of the α-CD hydroxyl groups to the solvent. To quantify the average distances observed between the two α-CDs of each of the three types of systems, radial distribution functions were calculated between all atoms of the first and the second α-CD (Fig. 10). In all three simulations carried out without implicit solvation, the smallest CDs interdistance is equal to 1.8 Å while it is equal to 4.4, 4.8, and 5.3 Å for solvated T–T, H–T, and H–H, respectively. The configurations obtained using the solvated models are thus closer to what is observed experimentally.

The most stable complexes of the non-solvated systems are the T–T complexes. This greater stability, around 27–30 kcal/mol with respect to the H–T and H–H, respectively, is due to more stable dipole–dipole and vdW energy terms, $E_{dip\text{–}dip\text{-}tot}$, and $E_{vdW\text{-}tot}$, respectively (Table 4). The weaker dipole–dipole interaction indicates a more favourable arrangement between the hydroxyl groups of the two adjacent secondary faces (tail) of the α-CDs than it appeared between the two primary faces in H–H complexes and between the secondary and primary faces of the H–T complexes. The T–T orientation of the CDs is in good agreement with what was observed for α-CDs dimers in vacuum by Bonnet et al. [25]. This indicates that the azobenzene chain has a weak impact on the orientation of the CDs. During the simulation of the T–T complex, the two α-CDs remained close to the centre of the chain. No translation toward the blocking groups was observed. In this situation, the α-CDs stay located in an energy well as already seen in the case of the [2]rotaxane. For the H–T complexes, the dimer formed by the two α-CDs was located close to a blocking group in the beginning of the dynamic, and later moved toward the centre of the chain, indicating that the α-CDs can cross the energy barrier localised between the two positions. Finally, for the H–H non-solvated model, the dimer was observed to be always located in an energy well close to the blocking group. These three different behaviours explain the differences in the $E_{vdW\text{-}tot}$ values. When an α-CD is placed next to a blocking group, the steric interaction is larger than when the α-CD is at the centre of the chain.

For the solvated systems, the T–T complexes are also the most stable as observed by Nascimento et al. for α-CDs dimers with water molecules [26]. However, the total average potential energy values of the two other solvated complexes are very close, ΔE = 1.4 and 4.1 kcal/mol for the H–H and H–T systems, respectively. Indeed, in the three solvated simulations, an α-CD remains next to the blocking group and does not interact significantly with the other CD. The $E_{vdW\text{-}tot}$ terms, that

Table 4
Average energy terms (kcal/mol) from the MD simulation of the head-to-head (H–H), head-to-tail (H–T), and tail-to-tail (T–T) [3]rotaxane complexes, carried out at 330 K, in the NVT ensemble, for a period of 102.5 ps, with and without implicit solvation, using the TINKER routine *Analyze* and MM3 force field

	H–H isolated state	H–T isolated state	T–T isolated state	H–H solvated state	H–H solvated state (1 ns)	H–T solvated state	T–T solvated state
E_{pot} [a]	419.8 ± 10.3	415.2 ± 10.2	388.3 ± 10.5	321.6 ± 9.9	328.1 ± 10.3	324.3 ± 10.2	320.2 ± 10.0
E_{kin} [a]	307.9 ± 10.2	307.9 ± 10.1	308.0 ± 10.1	307.9 ± 9.9	307.9 ± 10.2	307.9 ± 10.1	307.9 ± 10.0
E_{tot} [a]	727.7 ± 1.7	723.1 ± 1.9	696.2 ± 2.8	629.5 ± 1.3	636.0 ± 1.9	632.2 ± 1.2	628.1 ± 1.0
$E_{dip\text{–}dip\text{-}tot}$ [b]	−52.9 ± 3.2	−62.4 ± 5.2	−82.4 ± 3.2	−33.0 ± 2.9	−32.3 ± 2.8	−35.4 ± 2.6	−38.4 ± 2.9
$E_{vdW\text{-}tot}$ [b]	126.7 ± 8.0	117.5 ± 8.5	102.0 ± 8.1	135.4 ± 7.5	135.9 ± 7.8	133.6 ± 7.4	132.1 ± 7.5
E_{inter} [b]	−56.9 ± 4.1	−57.4 ± 3.5	−65.8 ± 4.2	−48.7 ± 2.7	−48.5 ± 2.9	−49.8 ± 2.8	−51.0 ± 3.3
E_{solv} [b]	–	–	–	−108.2 ± 1.6	−109.7 ± 2.2	−109.3 ± 1.8	−109.6 ± 2.0
$E_{non\text{-}solv}$ [c]	–	–	–	429.8	437.8	433.6	429.8

An additional MD of the solvated H–H [3]rotaxane complex was made with for a period of 1 ns.
[a] Average number calculated over all configurations.
[b] Average number calculated over saved configurations.
[c] Calculated as $E_{pot} - E_{solv}$.

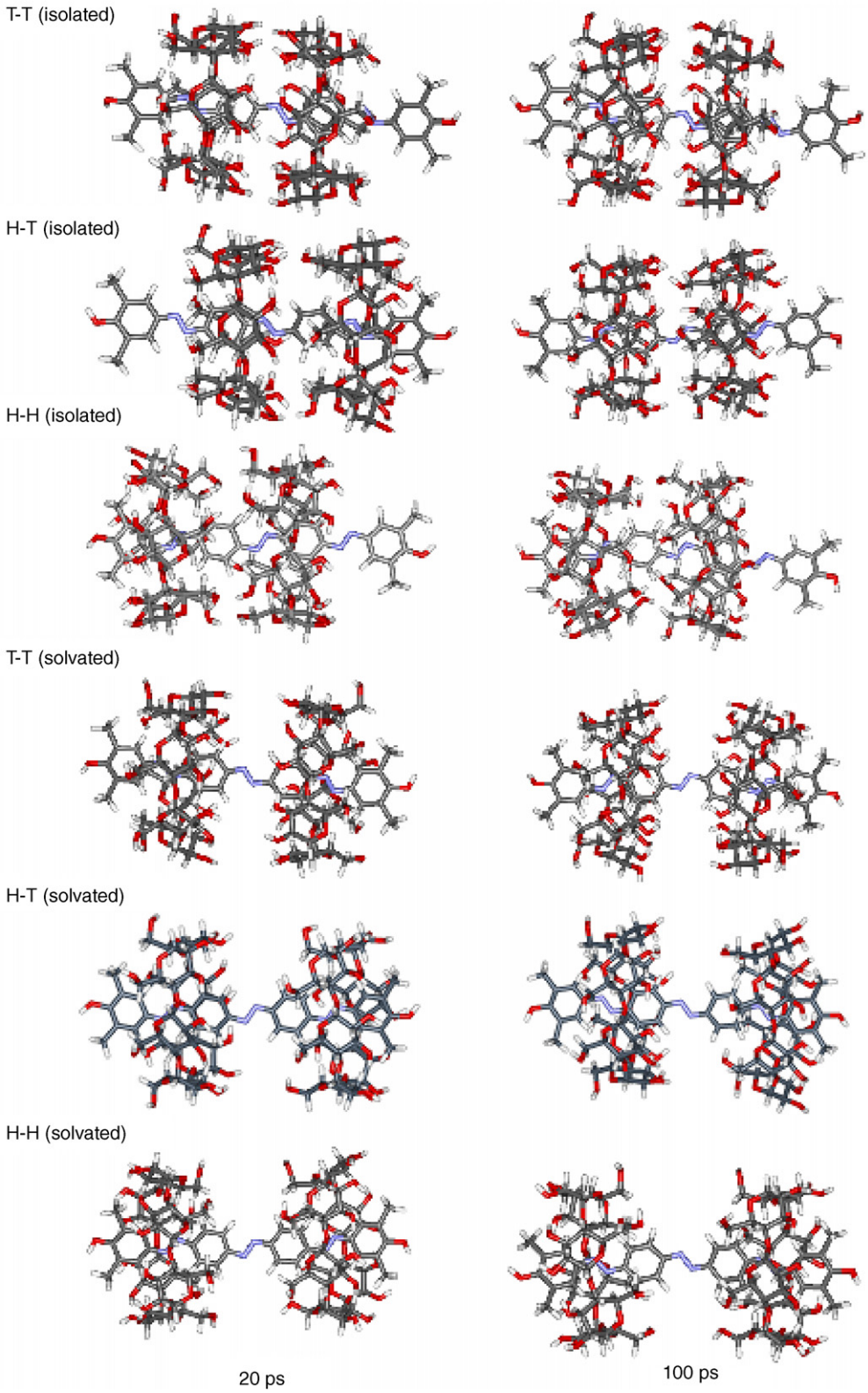

Fig. 9. Conformations adopted by the tail-to-tail (T–T), head-to-tail (H–T), and head-to-head (H–H) complexes of the α-CD/azobenzene [3]rotaxane at time step equal to 20 ps (left) and 100 ps (right) of the MD simulations carried out at 330 K, in the NVT ensemble, for a period of 102.5 ps, without and with implicit solvation, using the TINKER routine *Dynamic* and MM3 force field.

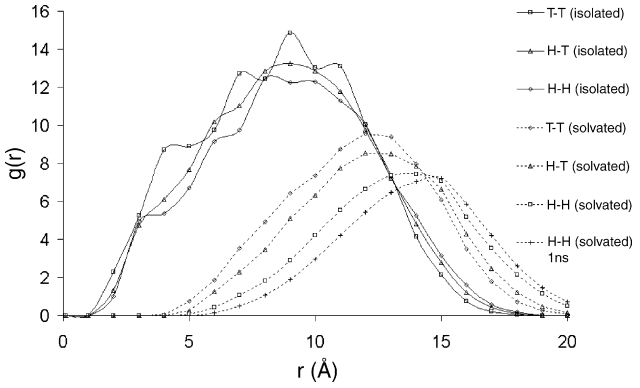

Fig. 10. Radial distribution functions between the atoms of the CDs calculated from the MD simulations of the tail-to-tail (T–T), head-to-tail (H–T), and head-to-head (H–H) complexes carried out at 330 K, in the NVT ensemble, for a period of 102.5 ps, with and without implicit solvation, using the TINKER routine *Dynamic* and MM3 force field.

characterize the interaction between the α-CDs and the guest chain, do not vary with the configuration of the complex, and the two α-CDs are too far away to present important electrostatic interactions between their mutual hydroxyl groups located on their primary or secondary faces. Thus, the total energy differences between the configurations of the system that depend on the relative orientation of the CDs are annihilated. The separation of the CDs is different from what it was observed for α-CDs dimers [23–26] but stays in agreement with Craig et al. conclusions [14].

It is well know that hydrogen bonds (H-bonds) are very important in CDs dimers [23]. So to estimate the cohesion between the two α-CDs in the isolated state and to evaluate the deformations of the α-CDs during the simulations, we analysed the properties of different types of H-bonds. It is usually accepted that strong, intermediate, and weak H-bonds correspond to 14–40 kcal/mol, 5–14 kcal/mol, and <5 kcal/mol, respectively [56]. Mean and standard deviation values of the number of H-bonds detected in windows of 20 snapshots are reported for each simulation in Table 5. First of all, no strong H-bond is observed in both isolated and solvated simulations. Secondly, less H-bonds are formed when solvation is included. In that case, no H-bonds between the two α-CDs (noted CD–CD in Table 5) can be formed because the distance between the two α-CDs is too large. The CDs are probably connected by H-bonds via water molecules, but as our model does not include explicit water molecule, this cannot be confirmed. Thirdly, several differences between the three isolated phase complexes are observed in the total number of H-bonds, principally due to the CD–CD H-bonds (Fig. 11). As observed previously [26], the T–T isolated phase complex possesses the larger number of both weak and intermediate CD–CD H-bonds, 17.2 ± 2.9 and 4.8 ± 1.8, respectively, due to a better arrangement of their mutual secondary hydroxyl groups. As each alcohol function could *a priori* form two H-bonds with the alcohol functions of the other α-CD, a maximum of 24 H-bonds could be formed between the two adjacent tails, *i.e.*, twice the number of hydroxyl groups in the secondary face. The high number of H-bonds leads thus to a larger stability for the dimer and leads to smaller E_{inter} and $E_{dip-dip-tot}$ values (Table 4). The two other isolated complexes are characterized by less numerous weak and intermediate CD–CD H-bonds, 10.2 ± 1.9 and 2.6 ± 1.4 for H–T, and 7.0 ± 1.9 and 2.1 ± 1.1 for H–H, respectively, because there are less primary hydroxyl groups on the tail, and the two α-CDs are slightly more distant (Fig. 10).

There is no significant difference between the numbers of weak intra-CD H-bonds. Most of them are due to H-bonds between secondary hydroxyls groups (OH_{sec}–OH_{sec}), that are located on the tail, and to H-bonds between hydroxyl groups of the head and ether oxygens (OH_{prim}–OH_{ether}). The average numbers of weak OH_{sec}–OH_{sec} H-bonds range between 11 and 12. These H-bonds are illustrated in Fig. 12 for the solvated H–H system. This indicates that each of the alcohol functions is oriented toward its nearest neighbour OH function in order to maximize the total dipole–dipole interaction.

Intermediate intra-CD H-bonds present a different behaviour. All of them are of OH_{sec}–OH_{sec} type, except for H–T and

Table 5
Average and standard deviation of the number of weak and intermediate hydrogen bonds calculated from MD calculations of the head-to-head (H–H), head-to-tail (H–T), and tail-to-tail (T–T) [3]rotaxane carried out at 330 K, in the NVT ensemble, for a period of 102.5 ps, with and without implicit solvation, using the TINKER routine *Dynamic* and MM3 force field

	H–H isolated state	H–T isolated state	T–T isolated state	H–H solvated state	H–T solvated state	T–T solvated state
Weak						
CD–CD	7.0 ± 1.9	10.2 ± 1.9	17.2 ± 2.9	–	–	–
OH_{sec}–OH_{sec}	11.4 ± 0.7	11.3 ± 0.8	11.7 ± 0.5	11.5 ± 0.6	11.5 ± 0.6	11.5 ± 0.7
OH_{prim}–OH_{prim}	0.9 ± 0.8	0.9 ± 1.1	0.6 ± 0.9	0.3 ± 0.5	0.6 ± 0.6	0.3 ± 0.4
OH_{prim}–OH_{ether}	9.2 ± 1.0	10.3 ± 1.7	9.9 ± 1.5	10.0 ± 1.4	10.1 ± 1.3	10.1 ± 1.2
OH–N	0.0 ± 0.3	0.9 ± 1.0	2.0 ± 1.9	–	–	–
Total	28.7 ± 2.8	33.1 ± 3.8	41.4 ± 3.6	21.7 ± 1.5	21.8 ± 2.2	21.4 ± 2.9
Intermediate						
CD–CD	2.1 ± 1.1	2.6 ± 1.4	4.8 ± 1.8	–	–	–
OH_{sec}–OH_{sec}	4.3 ± 1.2	4.3 ± 1.5	4.8 ± 1.0	3.5 ± 1.1	3.3 ± 3.5	3.6 ± 1.4
OH_{prim}–OH_{ether}	–	0.7 ± 1.2	0.9 ± 2.2	–	–	–
OH–N	–	0.5 ± 0.8	1.0 ± 1.3	–	–	–
Total	7.1 ± 1.7	7.9 ± 2.3	10.0 ± 4.3	3.5 ± 1.1	3.3 ± 1.1	3.9 ± 1.7

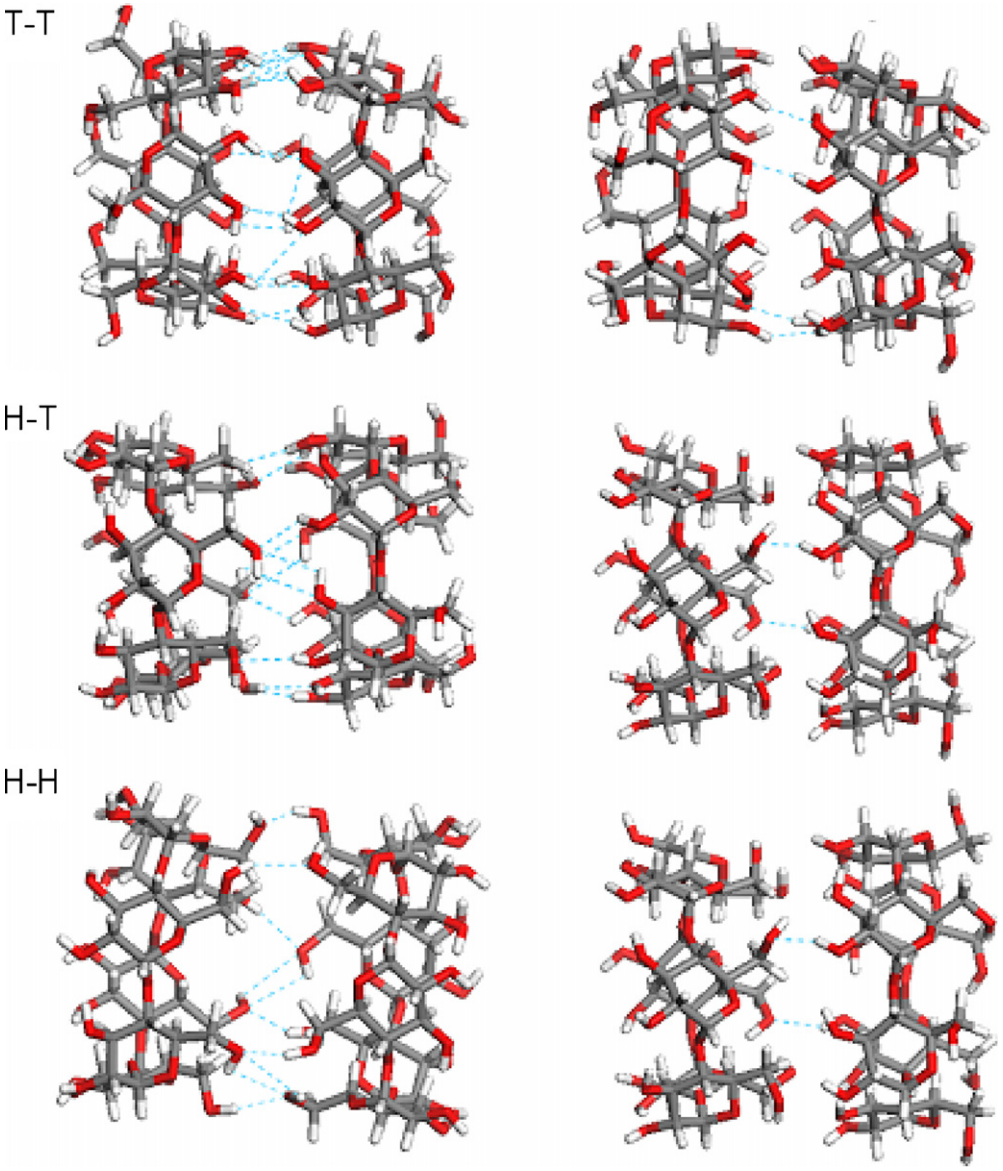

Fig. 11. Representation of the weak (left) and intermediate (right) CD–CD hydrogen bonds (dotted lines) between the α-CDs for the tail-to-tail (T–T), head-to-tail (H–T), and head-to-head (H–H) complexes without solvation. The snapshots were taken at time 50 ps of the MD simulation carried out at 330 K, in the NVT ensemble, for a period of 102.5 ps, using the TINKER routine *Dynamic* and MM3 force field.

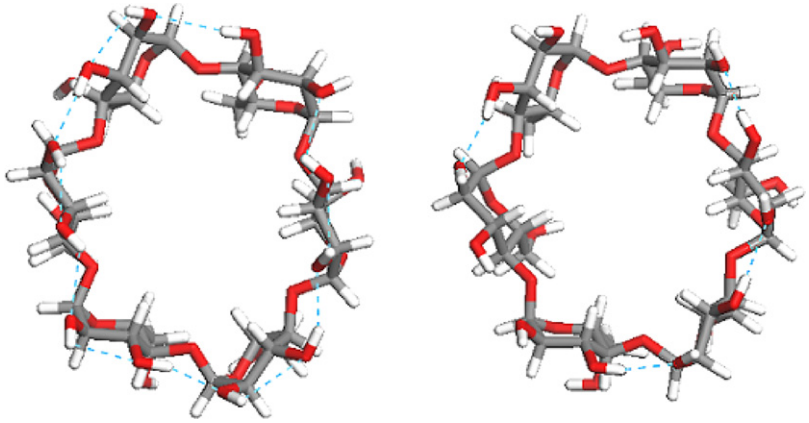

Fig. 12. Representation of the weak (left) and intermediate (right) OH_{sec}–OH_{sec} hydrogen bonds (dotted lines) as observed in an α-CD of the head-to-head complex modelled with implicit solvation at time 50 ps of the MD simulation carried out at 330 K, in the NVT ensemble, for a period of 102.5 ps using the TINKER routine *Dynamic* and MM3 force field.

T–T in the isolated state because few OH_{prim}–OH_{ether} and OH–N H-bonds are also observed. OH_{sec}–OH_{sec} H-bonds are formed by secondary hydroxyl groups of two adjacent glucoses of the α-CDs (Fig. 12) as described in literature [57]. Due to deformation of the α-CDs, the number of inter-glucosidic OH_{sec}–OH_{sec} are not equal to 6 as observed for α-CDs, but vary between 3.3 and 4.8 depending on the type of complex. We can also note that solvation tends to unfavour the formation of these inter-glucosidic H-bonds since the average number of intermediate OH_{sec}–OH_{sec} H-bonds in the solvated state is lower than in its isolated state.

To ensure that our results are valuable despite of the short simulation time (102.5 ps), an additional 1 ns MD simulation was carried out for the H–H complex with implicit solvation. The results did not vary significantly from those generated by the shorter simulations. The CDs are slightly more distant from each other. The minimal distance observed between the two CDs is equal to 5.8 Å *versus* 5.3 Å for the short time simulation (Fig. 10). The computed energies are also quite similar to the short time simulation and did not change our conclusions (Table 4). E_{pot} is only higher by 6.5 kcal/mol compared to the short simulation. That small difference comes from an internal deformation due to the proximity of the CDs with the blocking groups as $E_{dip–dip-tot}$, $E_{vdw-tot}$, and E_{inter} are identical for the two simulations.

4. Conclusions and outlook

In this paper, we have investigated several structural, energetic, and dynamical properties of a synthesised [3]rotaxane complex formed by two α-CDs and an azobenzene type chain [14]. We first focussed on the [2]rotaxane, *i.e.*, a complex with one α-CD and an azobenzene type guest, to assess the possibility of displacement of one α-CD along the chain. This was achieved by molecular mechanics using the program Tinker and the MM3 force field. Two high-energy (45.7 kcal/mol) barriers disallowing the decomplexation and two small barriers (10.1 kcal/mol) allowing the displacement of the α-CD along the chain were observed. The displacement of the α-CD along the guest chain was further confirmed by molecular dynamics (MD) simulations performed at the experimental temperature of 330 K. Then, MD runs on three configurations of the [3]rotaxane with or without implicit solvation have been carried out at the experimental temperature. It was observed that solvation separates the α-CDs and pushes them near the blocking groups. Without solvation, several hydrogen bonds (H-bonds), including strong electrostatic interactions, between the two α-CDs can be formed to create a dimer. For the solvated systems, the interactions between the faces of the α-CDs and the solvent are more important and the α-CDs move away to increase their solvent accessible surfaces, which leads to a configuration that is closer to the experimental one. Consequently, no inter-CDs H-bonds can be made between the α-CDs in the solvated state. In that state, intra-CD H-bonds appear between the secondary hydroxyl groups while, in the isolated state, the intra-CD H-bonds are formed between the primary alcohol functions and ether oxygen as well as between the secondary hydroxyl groups.

As several similar types of α-CD/azobenzene systems are known to show isomerisation processes and are used as molecular shuttle, it is planned, in further studies to investigate the isomerisation mechanisms. Our present results will enable us to define valuable starting geometries for further structural and electronic properties investigation by quantum mechanics.

Acknowledgments

LB thanks the FUNDP for his FSR research grant. NS thank the ''Fonds pour la formation à la Recherche dans l'Industrie et dans l'Agriculture'' (FRIA) for his PhD fellowship. Calculations were performed using the Interuniversity Scientific Computing Facility (ISCF), installed at the University of Namur (Namur, Belgium), for which the authors gratefully acknowledge the University of Namur and the financial support of the FNRS-FRFC and the 'Loterie Nationale' for convention number 2.4578.02. The authors thank the referees who made pertinent remarks, which enable to enhance the quality of the manuscript.

References

[1] V. Balzani, A. Credi, F.M. Raymo, J.F. Stoddart, Artificial molecular machines, Angew. Chem. Int. Ed. 39 (2000) 3348–3391.
[2] A. Harada, Cyclodextrin-based molecular machines, Acc. Chem. Res. 34 (2001) 456–464.
[3] C.A. Schalley, K. Beizai, F. Vögtle, On the way to rotaxane-based molecular motors: studies in molecular mobility and topological chirality, Acc. Chem. Res. 34 (2001) 465–476.
[4] M. Clemente-León, F. Marchioni, S. Silvi, A. Credi, Photoactive pseudorotaxanes and rotaxanes as artificial molecular machines, Synth. Met. 139 (2003) 773–777.
[5] P.L. Anelli, N. Spencer, J.F. Stoddart, A molecular shuttle, J. Am. Chem. Soc. 113 (1991) 5131–5133.
[6] P.R. Ashton, R. Ballardini, V. Balzani, A. Credi, K.R. Dress, E. Ishow, C.J. Kleverlaan, O. Kocian, J.A. Preece, N. Spencer, J.F. Stoddart, M. Venturi, S. Wenger, A photochemically driven molecular-level abacus, Chem. Eur. J. 6 (2000) 3558–3574.
[7] S.I. Jun, J.W. Lee, S. Sakamoto, K. Yamaguchi, K. Kim, Rotaxane-based molecular switch with fluorescence signaling, Tetrahedron Lett. 41 (2000) 471–475.
[8] A.M. Elizarov, S.-H. Chiu, J.F. Stoddart, An acid–base switchable [2]rotaxane, J. Org. Chem. 67 (2002) 9175–9181.
[9] C.A. Stanier, S.J. Alderman, T.D.W. Claridge, H.L. Anderson, Unidirectional photoinduced shuttling in a rotaxane with a symmetric stilbene dumbbell, Angew. Chem. Int. Ed. 41 (2002) 1769–1772.
[10] D.H. Qu, Q.C. Wang, J. Ren, H. Tian, A light-driven rotaxane molecular shuttle with dual fluorescence addresses, Org. Lett. 6 (2004) 2085–2088.
[11] D.R. Stewart, D.A.A. Ohlberg, P.A. Beck, Y. Chen, R.S. Williams, J.O. Jeppesen, K.A. Nielsen, J.F. Stoddart, Molecule-independent electrical switching in Pt/organic monolayer/Ti devices, Nano Lett. 4 (2004) 133–136.
[12] H. Murakami, A. Kawabuchi, R. Matsumoto, T. Ido, N. Nakashima, A multi-mode-driven molecular shuttle: photochemically and thermally reactive azobenzene rotaxanes, J. Am. Chem. Soc. 127 (2005) 15891–15899.
[13] S. Anderson, T.D.W. Claridge, H.L. Anderson, Azo-dye rotaxanes, Angew. Chem. Int. Ed. 36 (1997) 1310–1313.
[14] M.R. Craig, T.D.W. Claridge, M.G. Hutchings, H.L. Anderson, Synthesis of a cyclodextrin azo dye [3]rotaxane as a single isomer, Chem. Commun. 16 (1999) 1537–1538.

[15] J.J. Michels, M.J. O'Connell, P.N. Taylor, J.S. Wilson, F. Cacialli, H.L. Anderson, Synthesis of conjugated polyrotaxanes, Chem. Eur. J. 9 (2003) 6167–6176.
[16] J. Szejtli, Cyclodextrin Technology, Kluwer, Dordrecht, 1988.
[17] J.E.D. Davies (Ed.), Spectroscopic and Computational Studies of Supramolecular Systems, Kluwer, Dordrecht, 1992.
[18] K.B. Lipkowitz, Applications of computational chemistry to the study of cyclodextrins, Chem. Rev. 98 (1998) 1829–1874.
[19] F. Cramer, W. Saenger, H.-C. Spatz, Inclusion compounds. XIX. The formation of inclusion compounds of α-cyclodextrin in aqueous solutions. Thermodynamics and kinetics, J. Am. Chem. Soc. 89 (1967) 14–20.
[20] A.E. Kaifer, Interplay between molecular recognition and redox chemistry, Acc. Chem. Res. 32 (1999) 62–71.
[21] B. Pose-Vilarnovo, I. Perdomo-López, M. Echezarreta-López, P. Schroth-Padro, E. Estrada, J.J. Tores-Labandeira, Improvement of water solubility of sulfamethizole through its complexation with β- and hydroxypropyl-β-cyclodextrin—characterization of the interaction in solution and in solid state, Eur. J. Pharm. Sci. 13 (2001) 325–331.
[22] L. Leherte, T. Latour, D.P. Vercauteren, Topological analysis of electron density maps for chiral cyclodextrin–guest complexes: a steric interaction evaluation, Supramol. Sci. 2 (1995) 209–217.
[23] A. Wu, X. Shen, Y. He, Investigation on γ-cyclodextrin nanotube induced by *N*,*N*′-diphenylbenzidine molecule, J. Colloid Interf. Sci. 297 (2006) 525–533.
[24] I.N. Topchieva, A.E. Tonelli, I.G. Panova, E.V. Matuchina, F.A. Kalashnikov, V.I. Gerasimov, C.C. Rusa, M. Rusa, M.A. Hunt, Two-phase channel structures based on α-cyclodextrin–polyethylene glycol inclusion complexes, Langmuir 20 (2004) 9036–9043.
[25] P. Bonnet, C. Jaime, L. Morin-Allory, Structure and thermodynamics of α-, β-, and γ-cyclodextrin dimers. Molecular dynamics studies of the solvent effect and free binding energies, J. Org. Chem. 67 (2002) 8602–8609.
[26] C.S. Nascimento Jr., C.P.A. Anconi, H.F. Dos Santos, W.B. De Almeida, Theoretical study of the α-cyclodextrin dimer, J. Phys. Chem. A 109 (2005) 3209–3219.
[27] P. Bortolus, S. Monti, *Cis–trans* photoisomerization of azobenzene–cyclodextrin inclusion complexes, J. Phys. Chem. 91 (1987) 5046–5050.
[28] A.M. Sanchez, R.H. de Rossi, Effect of β-cyclodextrin on the thermal *cis–trans* isomerization of azobenzenes, J. Org. Chem. 61 (1996) 3446–3451.
[29] N. Yoshida, H. Yamaguchi, T. Iwao, M. Higashi, Induced circular dichroism spectra of α-, β-, and γ-cyclodextrin complexes with π-conjugate compounds. Part 2. Chiral dimer formation and polarization directions of π–π^* transitions in some hydroxyazo guests having a naphtalene nucleus, J. Chem. Soc., Perkin Trans. 2 (2) (1999) 379–386.
[30] Y. Liu, Y.-L. Zhao, Y. Chen, D.-S. Guo, Assembly behavior of inclusion complexes of β-cyclodextrin with 4-hydroxyazobenzene and 4-aminoazobenzene, Org. Biomol. Chem. 3 (2005) 584–591.
[31] L. Briquet, D.P. Vercauteren, E.A. Perpète, D. Jacquemin, Is solvated *trans*-azobenzene twisted or planar? Chem. Phys. Lett. 417 (2006) 190–195.
[32] D.J. Barbiric, E.A. Castro, R.H. de Rossi, A molecular mechanics study of 1:1 complexes between azobenzene derivatives and β-cyclodextrin, J. Mol. Struct. (Theochem.) 532 (2000) 171–181.
[33] D.J. Barbiric, R.H. de Rossi, E.A. Castro, Inclusion complexes of 1:2 stoichiometry between azobenzenes and cyclodextrins: a molecular mechanics study, J. Mol. Struct. (Theochem.) 537 (2001) 235–243.
[34] K. Sohlberg, B.G. Sumpter, D.W. Noid, Semi-empirical study of a prototype rotaxane-based molecular shuttle, J. Mol. Struct. (Theochem.) 491 (1999) 281–286.
[35] G. Castruonovo, V. Elia, D. Fessas, F. Velleca, G. Viscardi, Thermodynamics of the interaction of α-cyclodextrin with monocarboxylic acids in aqueous solutions: a calorimetric study at 25 °C, Carbohydr. Res. 287 (1996) 127–138.
[36] A. Gadre, V. Rüdiger, H.-J. Schneider, K.A. Connors, Binding of cyclodextrins to alicyclic and aromatic substrates: complex formation of α-, β-, and γ-cyclodextrins with substituted cyclohexanecarboxylic acids and phenylalkanoic acids, J. Pharm. Sci. 86 (1997) 236–243.
[37] A.C.S. Lino, Y. Takahata, C. Jaime, α- and β-cyclodextrin complexes *n*-alkyl carboxylic acids and *n*-alkyl *p*-hydroxy benzoates. A molecular mechanics study of 1:1 and 1:2 associations, J. Mol. Struct. (Theochem.) 594 (2002) 207–213.
[38] M.T. Faucci, F. Melani, P. Mura, Computer-aided molecular modeling techniques for predicting the stability of drug–cyclodextrin inclusion complexes in aqueous solutions, Chem. Phys. Lett. 358 (2002) 383–390.
[39] Y. Choi, S. Jung, Molecular dynamics simulations for the prediction of chiral discrimination of *n*-acetylphenylalanine enantiomers by cyclomaltoheptaose based on the MM-PBSA approach, Carbohydr. Res. 339 (2004) 1961–1966.
[40] X. Grabuleda, C. Jaime, Molecular shuttles. A computational study (MM and MD) on the translational isomerism in some [2]rotaxanes, J. Org. Chem. 63 (1998) 9635–9643.
[41] X. Grabuleda, P. Ivanov, C. Jaime, Computational studies on pseudorotaxanes by molecular dynamics and free energy perturbation simulations, J. Org. Chem. 68 (2003) 1539–1547.
[42] X. Grabuleda, P. Ivanov, C. Jaime, Shuttling process in [2]rotaxanes. Modeling by molecular dynamics and free energy perturbation theory, J. Phys. Chem. B 107 (2003) 7582–7588.
[43] Tinker 4.0, User's Guide, J.W. Ponder, 2003.
[44] F.H. Allen, The Cambridge structural database: a quarter of a million crystal structures and rising, Acta Crystallogr. B 58 (2002) 380–388.
[45] B. Klar, B. Hingerty, W. Saenger, Topography of cyclodextrin inclusion complexes. XII. Hydrogen-bonding in the crystal structure of α-cyclodextrin hexahydrate: the use of multicounter detector in neutron diffraction, Acta Crystallogr. B 36 (1980) 1154–1165.
[46] H.S. Freeman, S.A. Mc Intoch, P. Singh, X-ray crystal structure of diazo dyes. Part 2. Derivatives of C.I. disperse yellow 23 and C.I. disperse orange 29, Dye Pigm. 35 (1997) 149–164.
[47] Materials Studio, Getting Started, Version 2.2, Accelrys Inc., San Diego, 2002.
[48] N.L. Allinger, Y.H. Yuh, J.H. Lii, Molecular mechanics. The MM3 force field for hydrocarbons, 1, J. Am. Chem. Soc. 111 (1989) 8551–8566.
[49] J.A. Bouwstra, A. Schouten, J. Kroon, Structural studies of the system *trans*-azobenzene/*trans*-stilbene. I. A reinvestigation of the disorder in the crystal structure of *trans*-azobenzene, $C_{12}H_{10}N_2$, Acta Crystallogr. C 39 (1983) 1121–1123.
[50] A. Mostad, C. Roemming, Refinement of the crystal structure of *cis*-azobenzene, Acta Chem. Scand. 25 (1971) 3561–3568.
[51] H. Fliegl, A. Köhn, C. Hättig, R. Ahlrichs, *Ab initio* calculation of the vibrational and electronic spectra of *trans*- and *cis*-azobenzene, J. Am. Chem. Soc. 125 (2003) 9821–9827.
[52] V. Stepanić, G. Baranović, V. Smrečki, Structure and vibrational spectra of conjugated acids of *trans*- and *cis*-azobenzene, J. Mol. Struct. 569 (2001) 89–109.
[53] R. Czerminski, R. Elber, Reaction path study of conformational transitions in flexible systems: applications to peptides, J. Chem. Phys. 92 (1990) 5580–5601.
[54] S. Nakamura, H. Hirose, M. Ikeguchi, J. Doi, Conformational energy minimization using a two-stage method, J. Phys. Chem. 99 (1995) 8374–8378.
[55] D. Eisenberg, A.D. McLachlan, Solvation energy in protein folding and binding, Nature 319 (1986) 199–203.
[56] G.R. Desiraju, T. Steiner, The Weak Hydrogen Bond, Oxford Science Publication, 1999.
[57] G.A. Jeffrey, W. Saenger, Hydrogen Bonding in Biological Structures, Springer, Berlin, 1994.